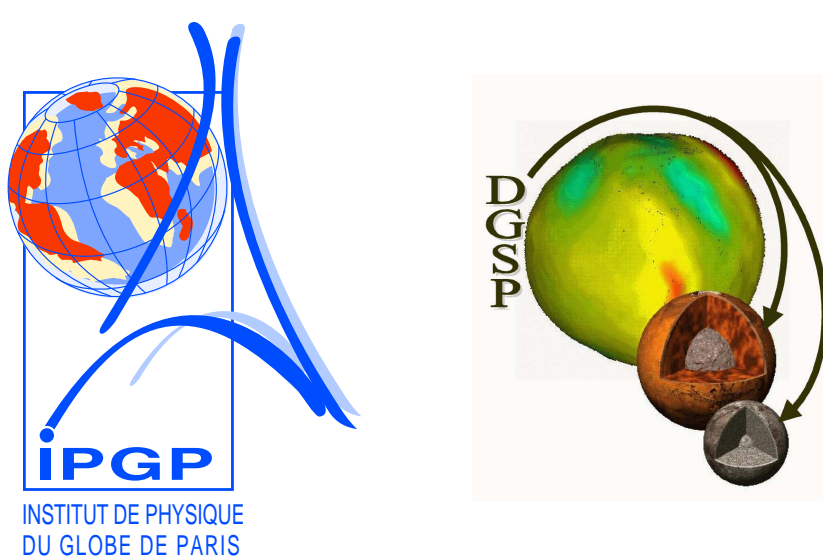


Non-linear waveform and delay time analysis of triplicated core phases

Raphaël Garcia^{1,2}, Sébastien Chevrot¹

e-mail : garcia@ipgp.jussieu.fr

¹ Laboratoire de Dynamique Terrestre et Planétaire, Observatoire Midi-Pyrénées, 14, Ave E. Belin 31400 Toulouse, France
² now at Département de Géophysique Spatiale et Planétaire, Institut de Physique du Globe de Paris, 4, Ave de Neptune, 94107 Saint Maur des Fossés, France



ABSTRACT

We introduce a new method to measure differential travel times and attenuation of seismic body waves. The problem is formulated as a non linear inverse problem which is solved by simulated annealing. Using this technique, we have analysed triplicated PKP waves recorded by the temporary EIFEL array in central Europe. These examples demonstrate the potential of the technique, which is able to determine differential traveltimes and waveforms of the core phases, even when they interfere

on the seismograms or when additional depth phases are present. The PKP differential travel times reveal the presence of large amplitude and small scale heterogeneities along the PKP(AB) ray paths, and favour an inner core model with 0.8% velocity perturbation in its top 150 km and small velocity perturbations below. The estimate of PKP differential attenuation puts a lower bound of 200 on the inner core quality factor in the top 300 km of the inner core.

INTRODUCTION

The arrival times of body waves are the primary source of information exploited in the seismological records. Large data sets have been created which allowed tomographic studies at both regional and global scales. The growth of data recorded by seismic networks during the past decade has motivated the search for new methods to measure routinely body wave arrival times. Classically, these methods are based on cross correlations between the different records of a network. Chevrot (2002) has described a non linear algorithm that permits the estimation of the optimal waveform recorded by all the stations of a seismological network, and its time delays at each station. While the analysis of seismograms contain-

ing a single prominent seismic phase is relatively simple, seismologists often face complex records where different seismic phases interfere. To demonstrate that the same approach can also be used on such records, we have generalized the algorithm to the case of interfering waves. We focus on the analysis of seismograms in the distance range of the PKP triplication. On these kind of records, interference is particularly strong. We invert for the reference waveform recorded by all the stations, and describe the other body waves as the attenuated and time shifted versions of this reference waveform. This approach therefore incorporates some a priori information in the inversion process.

METHOD

A priori information and model

Synthetic PKP phases are computed following the formula : $S_i(t) = \text{PKP}(\text{DF})(t) + \text{PKP}(\text{BC})(t) + \text{PKP}(\text{AB})(t)$
 $S_i(t) = R_{DF}A(t_i^*) * W(t + \tau_i^{DF}) + W(t + \tau_i^{BC}) + R_{AB}H * W(t + \tau_i^{AB})$
 where $S_i(t)$ is seismogram number i , $W(t)$ is the waveform of the PKP(BC) phase taken as reference, $A(t_i^*)$ is a differential attenuation operator, H is the Hilbert transform operator, R_{DF} and R_{AB} are real numbers standing for amplitude corrections, and τ_i^{DF} , τ_i^{BC} and τ_i^{AB} are the time shifts of the PKP(DF), PKP(BC) and PKP(AB) phases respectively, relative to the beginning of the record.

Optimization algorithm : Simulated Annealing

- minimize $E = \sum_i \int |D_i(t) - S_i(t)| dt$.
- exponential cooling schedule $T(k) = \gamma^k T(0)$ with $\gamma = 0.9$ and $N=300$ iterations.
- perturbation of the parameters with Cauchy probability parametrized with $T_j = \left(\frac{E(k)}{E(0)}\right)^\beta$.
- reannealing procedure to solve cycle skipping ambiguities.
- statistical study of 20 inversion results to estimate a posteriori covariance.

Acknowledgments

We thank Michael Weber, Martin Budweg and the EIFEL team for providing the core phase data, and for their technical support on this data set. This study has been partly supported by the program "Intérieur de la Terre" of INSU (Institut National des Sciences de l'Univers).

References

- Chevrot, S., 2002. Optimal waveform and delay time analysis by simulated annealing, *Geophys. J. Int.*, **151**, 164-171.
- Garcia, R., 2002. Constraints on upper inner core structure from waveform inversion of core phases, *Geophys. J. Int.*, **150**, 651-664.
- Ritter, J., Achauer, U., Christensen, U., and Eifel plume team, 2000. The teleseismic tomography experiment in the Eifel region, Central Europe : Design and first results, *Seism. Res. Lett.*, **71**, 55-62.

EXAMPLES OF APPLICATION

EIFEL Dataset

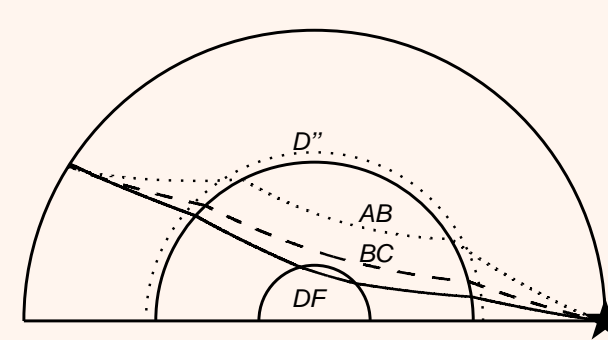


Figure 1 : Ray paths of the three PKP branches in the Earth : PKP(DF) (full line), PKP(BC) (dashed line) and PKP(AB) (dotted line). The event (black star) and the D" layer at the base of the mantle are also indicated.

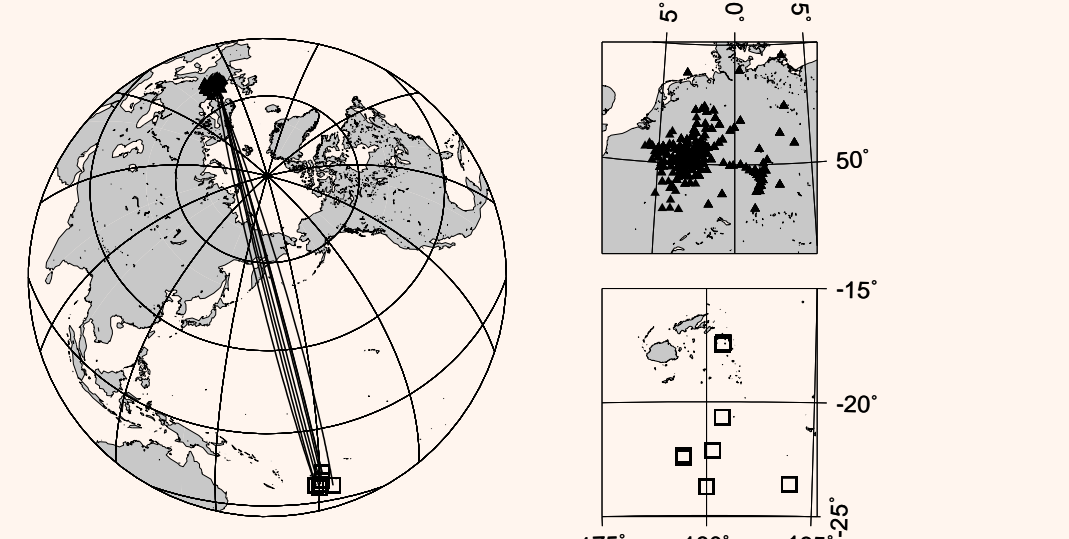


Figure 2 : On the left, stations (black triangles) and events (open squares) locations with typical great circle paths (full lines). On the right, zoom of the receiver (top) and source (bottom) regions.

3 PKP separated phases

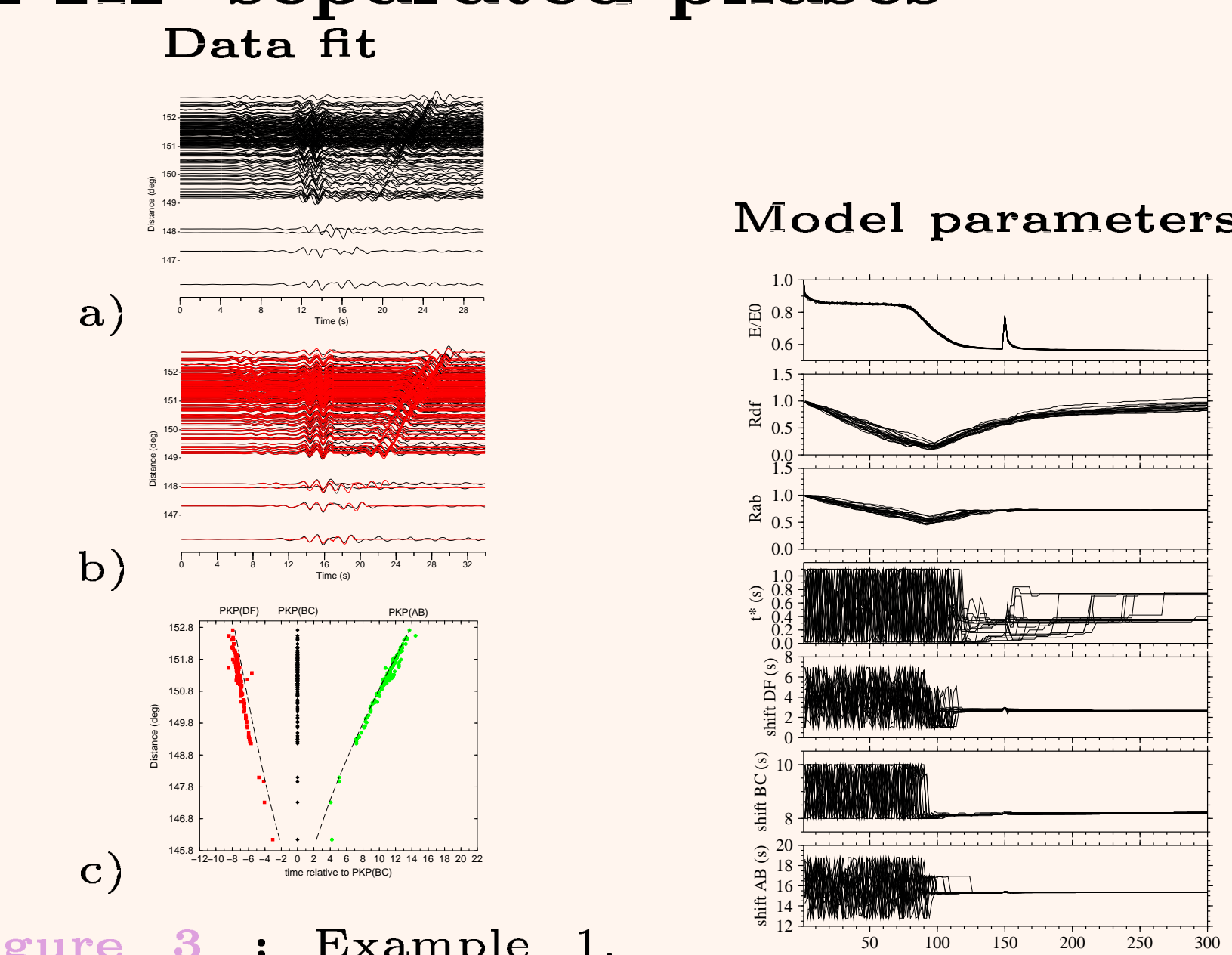


Figure 3 : Example 1. a) raw data, aligned on the theoretical arrival time of PKP(BC), as a function of epicentral distance (in degrees). b) data (black lines) and best model synthetic seismograms (red lines). c) arrival times of the three PKP phases relative to PKP(BC), and to AK135 Earth model (dashed lines).

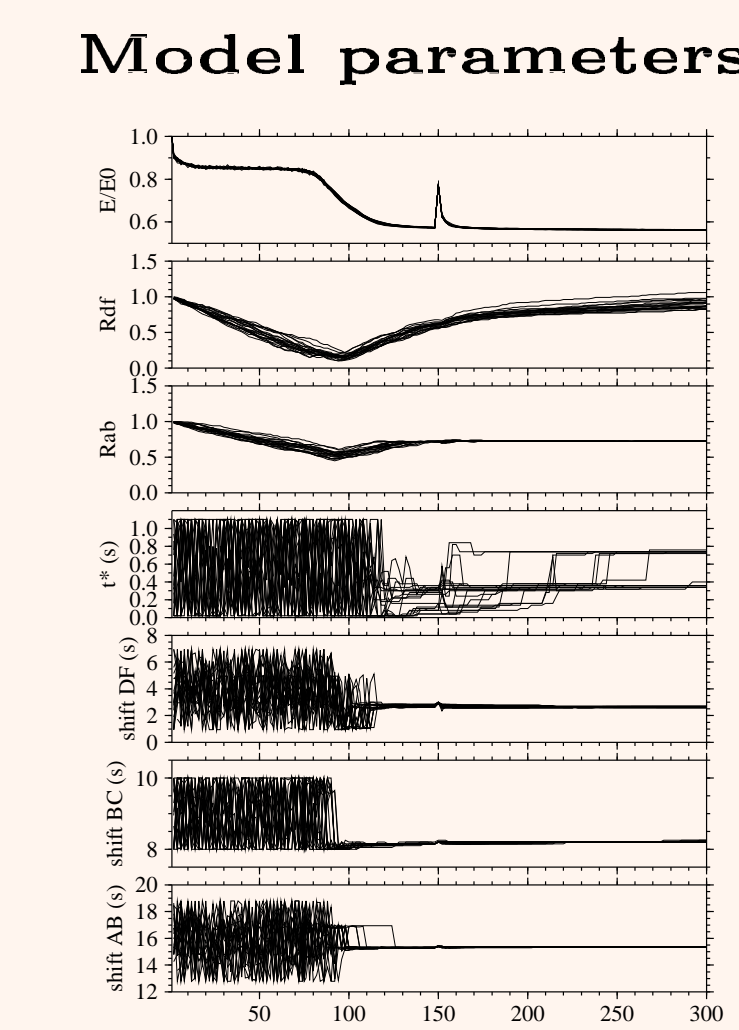


Figure 4 : Energy, R_{DF} , R_{AB} and parameters of a randomly selected seismogram, as a function of the temperature step (k) describing the cooling schedule.

Interfering PKP phases

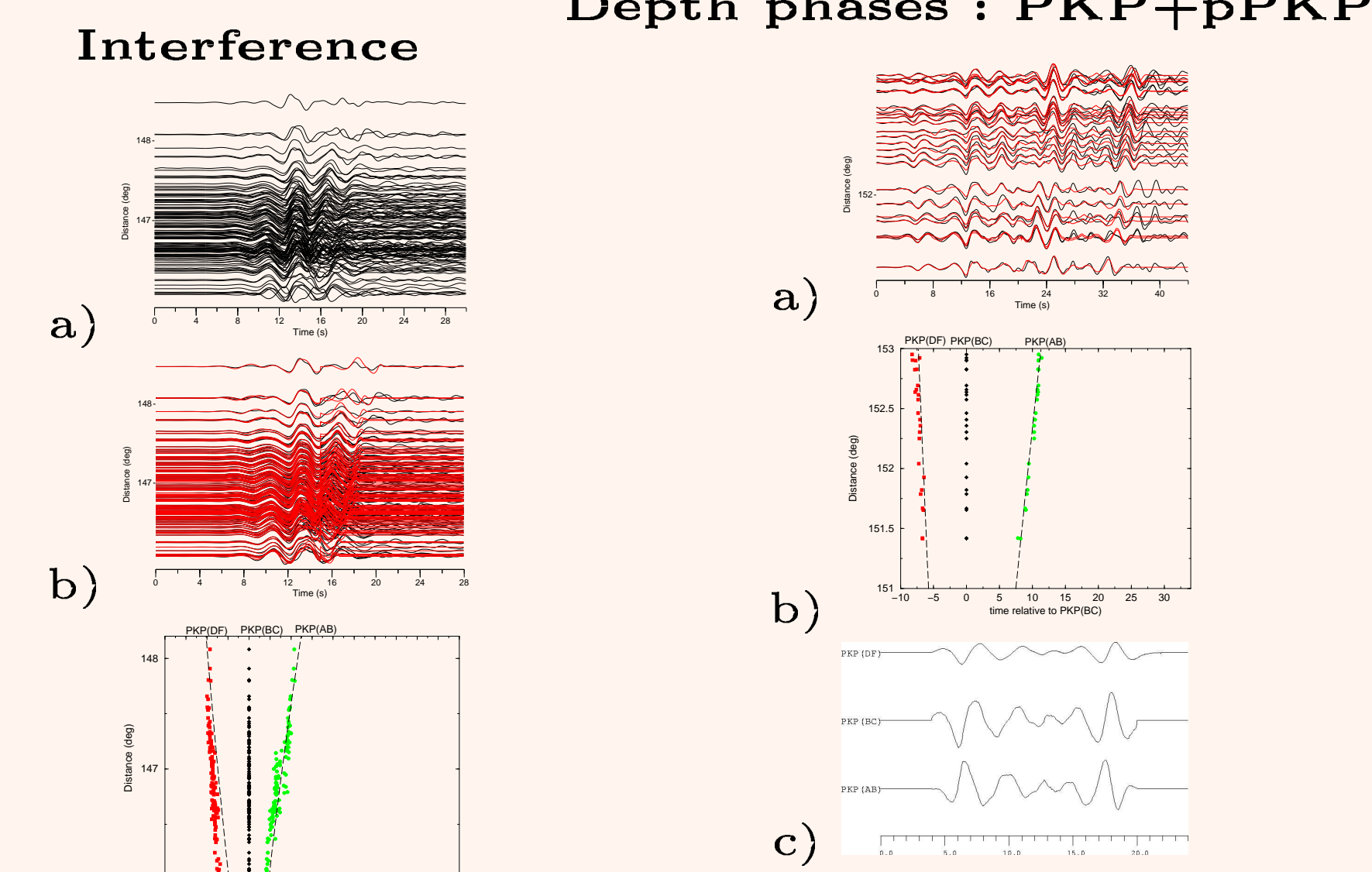


Figure 5 : Example 2. a) raw data, aligned on the theoretical arrival time of PKP(BC), as a function of epicentral distance (in degrees). b) data (black lines) and best model synthetic seismograms (red lines). c) waveforms obtained after inversions for the three PKP phases relative to PKP(BC), and to AK135 Earth model (dashed lines).

Figure 6 : Example 3. a) data (black lines) and best model synthetic seismograms (red lines). b) arrival times of the three PKP phases relative to PKP(BC), and to AK135 Earth model. (dashed lines) c) waveforms obtained after inversions for the three PKP phases relative to PKP(BC), and to PKP(AB) phases. Notice the two energy arrivals associated to direct and depth phases.

INNER CORE STRUCTURE

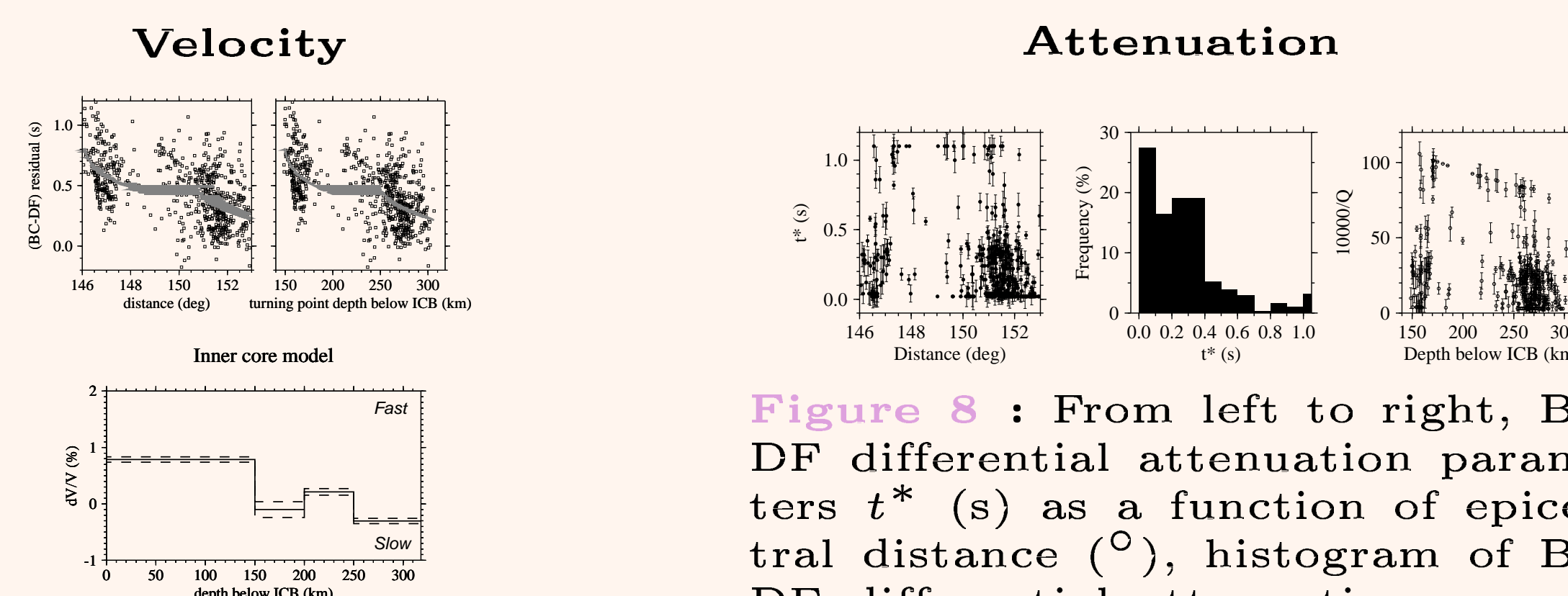


Figure 7 : BC-DF differential travel time residuals for the ak135 Earth model and corresponding inner core model.

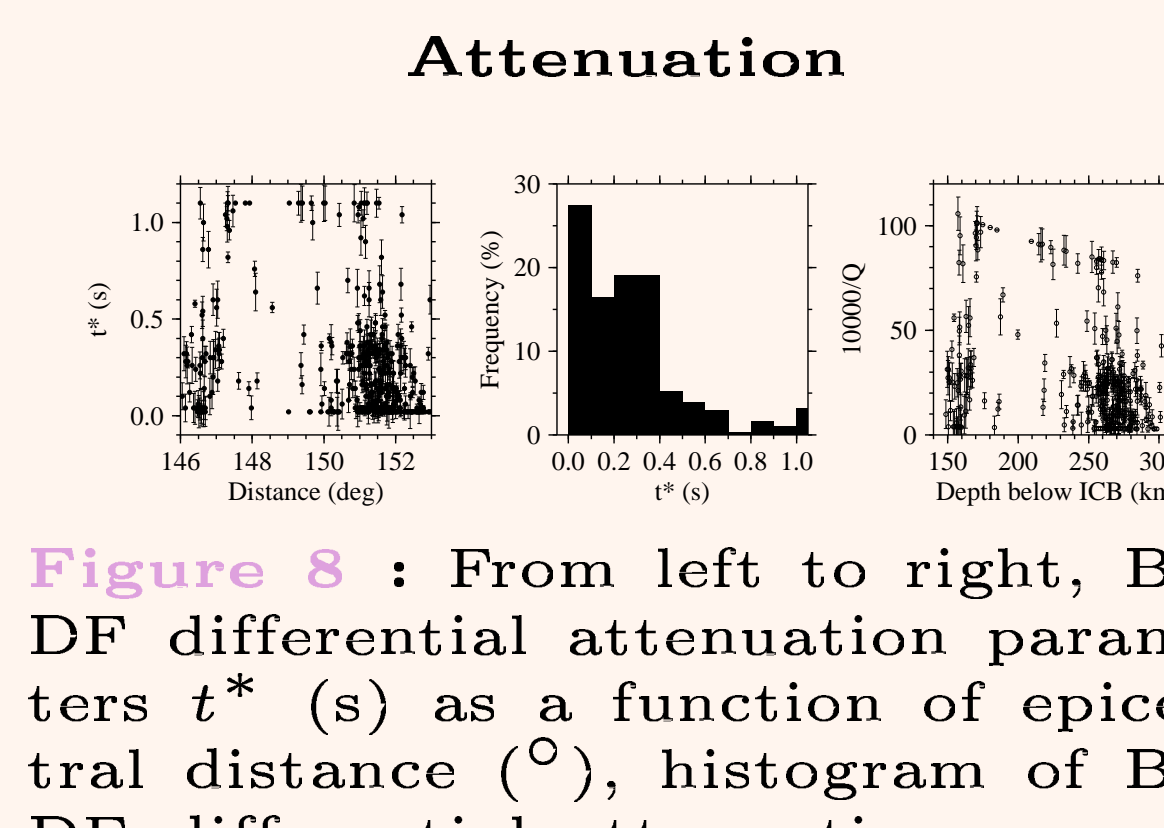


Figure 8 : From left to right, BC-DF differential attenuation parameters t^* (s) as a function of epicentral distance ($^\circ$), histogram of BC-DF differential attenuation parameters t^* , and inner core attenuation through the parameter $q=10000/Q$ as a function of PKP(DF) turning point depth in the inner core (km).

DISCUSSION

Advantages and limitations

- Advantages of the method :
- the method is **simple** and can be used **routinely and automatically**.
 - the search for a global minimum is successful even on **noisy data**.
 - the non-linear inversion algorithm allows to estimate waveforms and differential travel times **even when the three phases interfere on the seismograms**.
 - the waveform $W(t)$ can be used to estimate the source time function.
- The limitations come from the approximations used : simple source radiation and small waveform distortions produced by scattering.

Conclusions

The parametrized inversion described is very efficient to estimate relative arrival times and attenuations of seismic body waves, even when they interfere or when depth phases are present in the records. This approach opens new possibilities to study the fine structure of the inner core, the D" layer and the mantle discontinuities through the investigation of PKP and P triplications. The BC-DF differential attenuations put a lower bound of 200 on the average quality factor in the top 300 km of the inner core for this region, and for frequencies between 0.3 and 1.5 Hz.